

Melt Dynamics of Blended Poly(oxyethylene) Chains and Rings

Sunghyun Nam,[†] Johannes Leisen,[†] Victor Breedveld,[‡] and Haskell W. Beckham^{*†}

Polymer, Textile and Fiber Engineering, Georgia Institute of Technology, Atlanta, Georgia 30332-0295, and Chemical and Biomolecular Engineering, Georgia Institute of Technology, Atlanta, Georgia 30332-0100

Received October 13, 2008; Revised Manuscript Received March 5, 2009

ABSTRACT: Monodisperse cyclic poly(oxyethylene) (CPOE) was synthesized from linear dihydroxy-terminated poly(oxyethylene) (LPOE) with molecular weights from 400 to 1500 g/mol. Blends of CPOE with LPOE were prepared and examined with pulsed-field-gradient (PFG) ¹H NMR and rheology to determine the self-diffusion coefficient (*D*) and zero-shear viscosity (*η*) in the melt. Single average diffusion coefficients were measured for all blends. For blends prepared from components with equivalent molecular weights >400 g/mol, the *D*'s are suppressed and the *η*'s are enhanced in comparison with predictions based on binary mixing rules. This is attributed to topological threading of rings onto linear chains. Blends of perdeuterated LPOE with hydrogenous CPOE (1500 g/mol) were prepared and examined with PFG NMR. The resulting *D*'s, representing only the CPOE in the blends, are smaller than the average *D*'s measured for the fully hydrogenous blends at a given composition, indicating that complete averaging of the component molecular dynamics does not occur in these binary blends. Extrapolation to zero CPOE concentration yielded the trace *D* for 1500 g/mol CPOE in LPOE (2.8×10^{-12} m²/s at 56 °C). This trace *D*, assumed characteristic of threaded conformations, was used with the pure-component *D*'s and a three-term mixing rule to determine the percentage of rings threaded as a function of CPOE concentration. The results are in qualitative and quantitative agreement with published modeling studies.

1. Introduction

Very shortly after the first reports on the synthesis of polymer rings, their melt dynamics in blends with linear polymers were characterized. These studies were conducted in an attempt to understand the effect of topology on chain dynamics and to test whether the prevailing theory of chain dynamics, reptation, could be used to describe the motion of polymers without chain ends. Antonietti et al.¹ solution-blended 16 kg/mol fluorescently labeled cyclic polystyrene (PS) with unlabeled linear PS (110 kg/mol) and used a holographic technique to study the self-diffusion of rings in the melt. When the binary blend sample was isolated by precipitation from solution, a self-diffusion coefficient (*D*) of 10^{-11} cm²/s was measured. However, when the blend sample was prepared by slow evaporation of the solvent, no diffusion of the rings was observed, giving rise to an estimated $D < 10^{-14}$ cm²/s. This lack of mobility was attributed to *threading of the rings by chains* during sample preparation as the solution concentration slowly increased.

McKenna and Plazek² measured the zero-shear viscosity (*η*) of blends of cyclic and linear PS with similar molecular weights (~180 kg/mol) and found that the cyclic *η* increased rapidly on addition of small amounts of linear PS. The *η* increase between cyclic PS concentrations (ϕ_c) of 0.85 to 1 can be described by $\eta \sim \phi_c^{-5.6}$, which is much steeper than expected based simply on the weighted average viscosities of the linear and cyclic PS. They invoked ring threading to explain the enhanced viscosity increase. Similar results were reported by Roovers, who examined the effect on the melt viscosity of linear polybutadiene (PB) upon adding cyclic PB.³ He plotted the ratio of the blend viscosity to the viscosity of the pure linear component ($\eta_{\text{blend}}/\eta_l$) versus the cyclic PB concentration in the blend. The data revealed that the blend viscosity increased above that expected from the weighted average of the two pure components. When cyclic PB (40 kg/mol) was mixed with 20–25% linear PB, the blend viscosity was 10 times greater than that of the pure rings. The rapid increase in viscosity was

attributed to the “increased number of entanglements per chain”.³

Semlyen et al. prepared cyclic poly(dimethylsiloxane)s (PDMS) and examined the melt viscosities and self-diffusion coefficients for 50:50 blends of equivalent-molecular-weight cyclic and linear PDMS.^{4,5} They covered the molecular-weight (MW) range from 0.3 to 30 kg/mol and found that the viscosities of the blends were lower than expected for the samples with less than 100 backbone bonds and higher than expected for the higher-MW samples. At a ring size of about 150 backbone bonds (~5.6 kg/mol), the blend viscosity increases more steeply with MW than the predicted viscosity calculated from the two pure-component viscosities assuming pure additivity (i.e., the weighted average viscosity). Since this MW is still well below the critical entanglement molecular weight (*M_e*) for linear PDMS (17 kg/mol), they pointed out that this viscosity increase “cannot be due to ‘conventional’ molecular entanglements.”⁵ It was suggested that the increased viscosities were due to chain threading, consistent with an earlier observation that cyclic PDMS must have at least 38 bonds to allow threading by linear PDMS.⁶ They concluded, “The diffusion and viscosity data also support the occurrence of an entanglement, unrelated to the conventional type, which starts at the critical ring size.”⁵ For blends of cyclic and linear polymers, the apparent “occurrence of an entanglement, unrelated to the conventional type”, is an intriguing idea as entanglements constitute one of the primary concepts of polymer science.

Topological effects are also apparent in the self-diffusion behavior of cyclic and linear DNA. Robertson and Smith used fluorescent microscopy to track the motion of labeled cyclic or linear DNA in solutions of chains or rings as a function of molecular length and concentration.^{7,8} They refer to their four topologically distinct samples as linear tracers in chains (L–L), linear tracers in rings (L–C), cyclic tracers in chains (C–L), and cyclic tracers in rings (C–C) and find that $D_{C-C} > D_{L-C} > D_{L-L} > D_{C-L}$ at 1 mg/mL. They also report that D_{C-L} , in contrast to the *D* for the other three topological mixtures, decreases too steeply with increasing concentration to be described by reptation alone: “a process much slower than reptation governs that case”.⁷

* Corresponding author. E-mail: beckham@gatech.edu.

[†] Polymer, Textile and Fiber Engineering.

[‡] Chemical and Biomolecular Engineering.

Important insights into the structure of cyclic/linear melts have been provided by modeling studies. Cyclic polymers are collapsed in their melts compared to linear polymers of the same lengths.^{9,10} This has been confirmed by scattering experiments.¹¹ Linear polymers added to a melt of cyclic polymers may thread multiple rings,¹² allowing the rings to swell until they reach the same size as comparable-MW linear chains.^{9,13,14} Such swelling enhances ring–ring interactions, resulting in a “percolating entangled network” responsible for the suppression of the melt dynamics.¹⁵

Threading of linear chains through cyclic polymers has been experimentally proven by trapping of cycles in networks^{6,16} and on linear chains by polyrotaxanation.^{17,18} For example, end-linking α,ω -dihydroxy-terminated linear PDMS in the presence of cyclic PDMS leaves some fraction of the cyclic PDMS trapped in the resulting network. The percentage of cyclics trapped (i.e., threaded) increases as a function of cycle size in a sigmoidal fashion from zero when the number of cyclic backbone atoms (n_r) is less than 38 to reach 94% at $n_r = 517$.⁶ These data have been successfully modeled with rotational isomeric state and Monte Carlo methods.^{19,20} Monte Carlo simulations have also been conducted to investigate the threading of cyclic POE by linear α,ω -dimethoxy-POE in the melt.¹² Specifically, this study examined the effect of ring sizes between 352 (24-crown-8) and 880 g/mol (60-crown-20) for a constant cyclic mass fraction of 0.25 and the effect of cyclic mass fraction from 0.1 to 0.75 for a constant ring size of 616 g/mol (42-crown-14). The major conclusions from this work were the following: cyclic/linear POE blends do not segregate, the fraction of threaded POE cyclics increases from <1% when the ring size is ≤ 440 g/mol to about 21% when the ring size is 880 g/mol, and multiple threading occurs for rings ≥ 616 g/mol. At low cyclic concentrations, the predominant multiple-threading event is a single ring threaded by multiple linear chains; at high cyclic concentrations, single linear chains threaded through multiple cycles are more likely.

Thus, topological threading occurs and affects melt dynamics in blends of cyclic and linear macromolecules. Such threading effects are interesting but have also been cited^{21,22} as an impediment to quantitative modeling of the dynamics of (presumably) pure cyclic polymers, as small fractions of linear contaminants significantly affect dynamics^{2,23} and are very difficult to remove. To better understand topological threading, we synthesized highly pure cyclic POE (400–1500 g/mol), prepared a series of blends with linear POE, and examined the melt dynamics of the blends with NMR self-diffusion and zero-shear viscosity measurements. Poly(oxyethylene) was chosen as the subject of these studies for a variety of reasons: (1) cyclic POE can be prepared and purified in high yield;²⁴ (2) linear POE is characterized by a relatively low entanglement molecular weight ($M_e \sim 2$ kg/mol)²⁵ and critical molecular weight for entanglement ($M_c \sim 5.87$ kg/mol),²⁵ which means that unentangled and entangled (according to the standard definitions) regimes can be studied without synthesizing high-MW cycles with all of their attendant difficulties in purification; (3) POE is a melt above 50–70 °C (depending on MW), thereby allowing dynamics measurements at relatively low and experimentally accessible temperatures; and (4) the melt dynamics of cyclic POE or its blends had not yet been reported. The influences of molecular weight and composition on the melt dynamics in blends of POE chains and rings are reported and compared with literature reports on other cyclic/linear blends.

2. Experimental Details

2.1. Materials. All starting materials and solvents were purchased from Aldrich and used without further purification. The synthesis of monodisperse cyclic poly(oxyethylene) (CPOE) from linear

dihydroxy-terminated poly(oxyethylene) (LPOE) ($M_n = 400, 600, 900$, and 1500 g/mol; $M_w/M_n = 1.01$) has been described in the literature.^{24,26} Briefly, end-to-end coupling of deprotonated LPOE in dilute solution via a tosylate intermediate gives CPOE with only oxyethylene repeat units. Removal of linear byproducts by inclusion complexation with α -cyclodextrin (α -CD) and fractional precipitation yields highly pure CPOE (yields = 50–75%, $M_w/M_n = 1.02$ –1.05) according to GPC and ¹H NMR. At room temperature, the pure CPOE was a clear liquid for 400 and 600 g/mol and a white waxy solid for 900 and 1500 g/mol.

Limited investigations were also conducted using LPOE and CPOE of 3.4 and 8 kg/mol. These CPOEs, unlike the ones described above, were prepared by ring closure of deprotonated dihydroxy-terminated LPOE in dilute dichloromethane to give CPOEs with backbone acetal linkages.²⁷ The LPOE ($M_w/M_n = 1.15$ for 3.4 kg/mol) was dissolved in CH₂Cl₂ and syringe-pumped over 48 h into a stirred suspension of KOH in CH₂Cl₂/hexane (65/35 v/v). After stirring for an additional 24 h, the reaction mixture was filtered; the crude product was obtained after rotary evaporation of the filtrate. The product was purified by dissolving in toluene and adding hexane to precipitate byproduct. The final 3.4 kg/mol cyclic product (yield $\sim 90\%$, $M_w/M_n = 1.19$) was a white powder and highly pure according to GPC.

Perdeuterated linear dihydroxy-terminated poly(oxyethylene) (d-LPOE, $M_n = 1600$ g/mol; $M_w/M_n = 1.32$) was purchased from Polymer Source, and 18-crown-6 was included in the study as another CPOE. The d-LPOE was mixed with 1500 g/mol CPOE to prepare a partially deuterated binary blend. While the d-LPOE has a slightly higher molecular weight (1600 g/mol), it is approximately the same average length as the 1500 g/mol CPOE with 33–34 repeat units. All samples were dried under high vacuum for days prior to use.

Binary blends were prepared by solution mixing in methanol (1 wt % polymer). Both polymers of a given blend composition were dissolved in methanol separately, mixed, and sonicated for 15 min. The solvent was then removed initially by rotary evaporation and finally under high vacuum. All blended samples, including those prepared from perdeuterated LPOE and hydrogenous CPOE, formed clear solutions and melts. Blends of perdeuterated and hydrogenous polymers can be immiscible, characterized by small positive interaction parameters and upper critical solution behavior.²⁸ On the other hand, blends of cyclic and linear polymers can also exhibit increased miscibility due to the entropy gained when freely interpenetrating linear chains are mixed with topologically restricted rings.^{9,29} The appearances and diffusion results of the d-LPOE/CPOE mixtures are consistent with those of miscible blends. All blended samples were kept above the melting temperatures of both components under vacuum for 48 h prior to any measurements.

2.2. NMR Measurements. All NMR experiments were performed on a magnetic resonance analyzer (MARAN 23 Ultra), operating at a ¹H frequency of 23 MHz using a permanent magnet. The spectrometer was equipped with a gradient probe and a Techtron gradient amplifier. A minimum of 280 mg of sample was measured in a 10 mm probe at a constant temperature of 56 °C, at which temperature all POE samples are melts.

The self-diffusion coefficient, D , was measured using a standard pulsed-field-gradient pulse sequence.³⁰ Stimulated echoes were produced from radio-frequency pulses in conjunction with a pair of gradient pulses. The normalized echo signal intensity for samples with two components diffusing independently at different rates is given by

$$\frac{I(\delta)}{I(0)} = w_1 \exp\{-XD_1\} + w_2 \exp\{-XD_2\} \quad (1)$$

where δ is the gradient pulse duration, w_1 and w_2 are the fractions of the two components ($w_1 + w_2 = 1$), D_1 and D_2 are the self-diffusion coefficients of the two components, and $X = \gamma^2 g^2 \delta^2 (\Delta - \delta/3)$ which includes the following PFG parameters: g is the gradient pulse magnitude, Δ is the gradient pulse separation or diffusion duration, and γ is the magnetogyric ratio of the nucleus being

Table 1. Self-Diffusion Coefficients of CPOE, LPOE, and Their 50:50 Blends at 56 °C^a

	<i>D</i> (m ² /s)			
	400 g/mol	600 g/mol	900 g/mol	1500 g/mol
CPOE	4.8×10^{-11}	3.4×10^{-11}	2.1×10^{-11}	8.8×10^{-12}
50:50 blend	4.2×10^{-11}	2.6×10^{-11}	1.3×10^{-11}	6.6×10^{-12}
LPOE	3.7×10^{-11}	2.4×10^{-11}	1.3×10^{-11}	7.3×10^{-12}

^a Standard deviations range from 5–10% for CPOE, 1–6% for the blends, and 1–3% for LPOE.

observed (¹H in these experiments). The gradient pulse magnitude *g* was set to achieve echo attenuation below at least 20% of the original signal intensity when varying δ from 0.5 to 3 ms in 20 increments. The largest value of *g* used in these studies was 2.28 T/m. The gradient pulse separation Δ was 100 ms, and the recycle delay was 1 s. For this diffusion duration (100 ms), diffusion distances $(2\Delta D)^{1/2}$ for the POEs examined here (cf. Table 1) are $>1 \mu\text{m}$, sufficiently large to ensure that center-of-mass diffusion is measured for all samples. *I*(δ) is the integrated peak intensity, and *I*(0) is the intensity when δ is equal to 0. The gradients were calibrated using water and its known *D*. For the fully hydrogenated blends, 32 scans provided sufficient signal-to-noise ratios. For the partially deuterated d-LPOE/CPOE blends, the number of scans was increased to 512 for the 40% and 60% and to 1024 for the 10% and 20% CPOE samples to compensate for the smaller number of signal-producing molecules in the sample. All data could be fitted to a single exponential decay ($w_2 = 0$ in eq 1). The average value of two *D* measurements on each sample is presented.

2.3. Viscosity Measurements. The viscosity (η) was measured with a MCR 300 rotational rheometer from Anton Paar using a cone and plate geometry. The diameter and angle of the stainless steel cone were 25 mm and 2°, respectively, with a sample volume of 140 μL . The viscosities of all samples were found to be constant for shear rates from 5 to 300 s^{−1}, and the zero-shear viscosity for each sample was therefore determined as the average of five η values at different shear rates. The measurements were carried out at 56 °C to enable direct comparison with the NMR data. Duplicate measurements were performed, and their average is presented.

3. Results and Discussion

3.1. Effect of Molecular Weight. The melt dynamics have recently been reported for pure CPOE and LPOE with molecular weights from 400 to 1500 g/mol.²⁶ At 56 °C, the self-diffusion coefficients are larger and the zero-shear viscosities are smaller for CPOE than for LPOE with the same molecular weight. The calorimetric glass transitions were also reported. The *T*_g's are similar but slightly higher (2–3 K) for CPOE at a given molecular weight. Thus, for experiments conducted at 56 °C, the CPOE samples are slightly closer to their *T*_g's. Since the CPOE exhibits the higher mobility (smaller η 's and larger *D*'s) despite being closer to its *T*_g, the differences in melt dynamics were attributed to chain-end and topological effects.

Blends of LPOE and CPOE were prepared by solution mixing. Typical spin–echo attenuation plots are shown in Figure 1 for blends containing equal weights of CPOE and LPOE at the same molecular weight. All the blends show single-exponential decays, signifying the presence of a single characteristic diffusive process. The self-diffusion coefficients, determined from the slopes of these spin–echo attenuation plots using eq 1 (with $w_2 = 0$), are listed in Table 1 along with the values for the pure CPOE and LPOE melts.

For a given molecular weight, the self-diffusion coefficient of pure CPOE is consistently higher than that of pure LPOE by an average factor of 1.4 ± 0.1 at 56 °C, indicating that the mobility of LPOE is lower than for CPOE with the same number of backbone atoms. Dynamic averaging is expected to occur in miscible blends^{5,31} so that the ratio of CPOE to LPOE diffusion coefficients should be even smaller than 1.4 in the blends. Such small differences in diffusion coefficients cannot be resolved

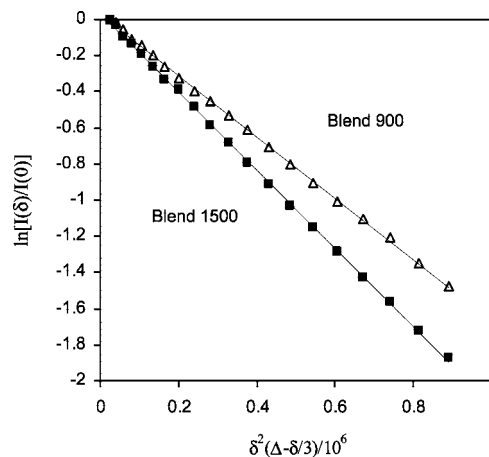


Figure 1. Spin–echo attenuation plots for two 50:50 (w/w) blends of CPOE and LPOE of equal molecular weight, respectively 900 (*g* = 1.37 T/m) or 1500 g/mol (*g* = 1.98 T/m), measured at 56 °C. Lines represent the fit of eq 1 with $w_2 = 0$, signifying the presence of one characteristic diffusion process.

in PFG diffusion data, as is illustrated in Figure 2. The figure shows simulated echo attenuation plots for a 50:50 blend in which the ratio of cyclic to linear diffusion coefficients (*D*_c/*D*_L) is 1.4 and 2, respectively. While two separate decay processes are detectable for *D*_c/*D*_L = 2, albeit only for very high-quality data, two diffusion processes are certainly not distinguishable when *D*_c/*D*_L ≤ 1.4. Thus, the appearance of a monoexponential PFG echo decay (e.g., as in Figure 1) does not necessarily signify that the dynamics of the individual blend components have been completely averaged. For a binary blend, a binary mixing rule can be used as first-order estimate of the detected blend diffusivity:

$$D_{\text{blend}} = w_1 D_1 + (1 - w_1) D_2 \quad (2)$$

where w_1 is the weight fraction of the component with diffusion coefficient *D*₁ and *D*₂ is the diffusion coefficient of the second component. This simple mixing rule has been used successfully to predict the diffusion coefficients for binary blends of poly(propylene oxide)s of different molecular weights (425–2000 g/mol).³² It also correctly predicts the *D* for our CPOE/LPOE blend at the lowest molecular weight of 400 g/mol (4.2×10^{-11} m²/s; cf. Table 1). However, the simple model clearly fails to capture the blend diffusivity for the higher-molecular-weight CPOE/LPOE blends. As shown in Table 1, the *D*_{blend} approaches the slower component (i.e., LPOE) with increasing molecular weight and becomes even smaller than the slow, linear component diffusivity for the 1500 g/mol blend. Similar results were also observed in blends of cyclic and linear PDMS,⁵ where the *D*_{blend} was found to be smaller than the diffusivity of both pure components with more than 200 skeletal bonds. This anomalous reduction in dynamics for sufficiently large cycles was attributed to topological threading, which apparently occurs in blends of cyclic and linear POE as well.

As described in the Introduction, topological threading was shown to also affect viscosities in blends of cyclic and linear PDMS.⁴ The viscosities of the CPOE/LPOE 50:50 blends (w/w) were measured as a function of shear rate from 5 to 300 s^{−1}. These data are shown in Figure 3 for the 400 g/mol blend, which does not exhibit threading effects in its diffusion behavior, and the 1500 g/mol blend, which does. Both samples exhibit Newtonian behavior. Thus, unlike conventional entanglements of linear chains, threaded entanglements are not apparent in the shear dependence of the viscosity at moderate shear rates.

The zero-shear viscosities for CPOE, LPOE, and their 50:50 blends are listed in Table 2. In good agreement with the diffusion

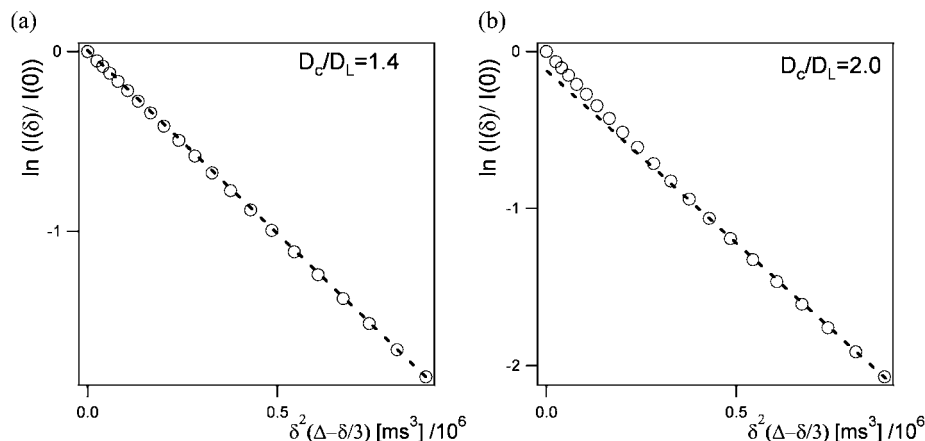


Figure 2. Simulated echo attenuation plots for a 50:50 blend in which the ratio of self-diffusion coefficients for cyclic and linear species (D_c/D_L) is (a) 1.4 and (b) 2. Equation 1 was employed with the same PFG parameters as those used to measure the experimental curves shown in Figure 1. The dashed line illustrates whether biexponential behavior is detectable in the data.

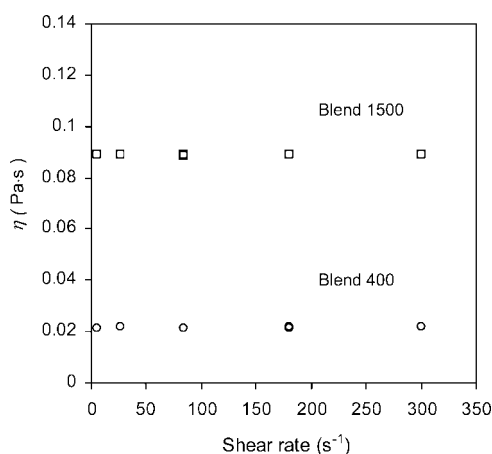


Figure 3. Viscosity vs shear rate at 56 °C for 50:50 blends (w/w) of CPOE and LPOE at the same molecular weight: 400 or 1500 g/mol.

Table 2. Zero-Shear Viscosities of CPOE, LPOE, and Their 50:50 Blends at 56 °C^a

	η (Pa·s)			
	400 g/mol	600 g/mol	900 g/mol	1500 g/mol
CPOE	0.018	0.026	0.039	0.064
50:50 blend	0.022	0.034	0.053	0.089
LPOE	0.024	0.036	0.059	0.093

^a Standard deviations range from 5–9% for CPOE, 5–7% for the blends, and 3–9% for LPOE.

data, the η_{blend} is very near the weighted average of the two pure components at 400 g/mol and approaches the slow component value (i.e., LPOE) with increasing molecular weight. Using a simple binary mixing law similar to eq 2 in which the D 's are replaced with η 's, viscosities were calculated for comparison with the experimental values. These are plotted in Figure 4 as $\eta_{\text{blend}}/\eta_{\text{calc}}$ versus number of skeletal bonds along with the analogous data for 50:50 blends of equivalent-molecular-weight cyclic and linear PDMS obtained from the literature.⁴ The similarity in the shapes of the two data sets for different polymers is striking. For the cyclic/linear PDMS blends, the higher-than-predicted viscosity values (i.e., $\eta_{\text{blend}}/\eta_{\text{calc}} > 1$) above 100 backbone bonds were attributed to topological threading.^{4,5} Topological threading is also apparent in the viscosity data for CPOE/LPOE blends. The threading onset occurs at a lower number of skeletal bonds for the CPOE/LPOE blends since POE does not have any side groups. Consistent with published Monte Carlo simulations of cyclic/linear POE blends,¹² threading occurs for molecular weights

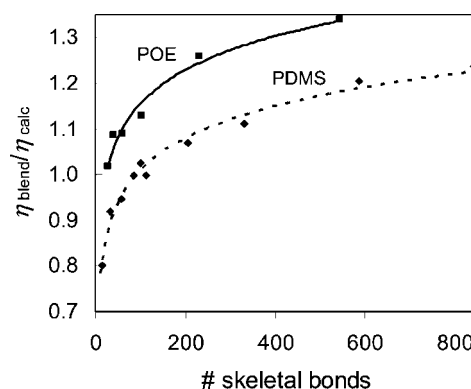


Figure 4. Ratios of experimental viscosities (η_{blend}) to viscosities calculated from the pure-component viscosities using a binary mixing rule (η_{calc}) vs number of skeletal bonds for 50:50 blends of cyclic and linear POE (■) and PDMS (◆). The PDMS data were taken from the literature.⁴

greater than 400 g/mol (27 skeletal bonds). Unlike the diffusion data in which $D_{\text{blend}} < D_{\text{LPOE}}$ for the 1500 g/mol blend, the η_{blend} is not greater than the η_{LPOE} for any of the blends. Thus, although the self-diffusion behavior indicates dynamics are reduced below that of the pure slow component due to topological threading, this does not result in viscosities greater than the viscosity of the pure slow component.

3.2. Effect of Composition. Figure 5 displays the self-diffusion coefficients for equi-MW CPOE/LPOE blends as a function of CPOE weight fraction for three different MW's: 400, 900, and 1500 g/mol. The data are plotted as the ratio of the measured average D of the blend, D_{blend} , to the D of the corresponding linear POE, D_{LPOE} , versus concentration of cyclic POE in the blend. For the smallest POE (400 g/mol), D_{blend} changes linearly with concentration of cyclic POE, as predicted by the binary mixing rule of eq 2 (dashed line in Figure 5) and consistent with observations for blends of small (i.e., 8–16 carbons) cyclic and linear alkanes.³¹ This observation indicates that the 400 g/mol cyclics are not large enough to be threaded by linear chains in the melt. In sharp contrast, the D_{blend} of the higher-MW blends (900 and 1500 g/mol) drops below the values predicted by a simple mixing rule. Starting with pure linear POE, translational dynamics of the blend are suppressed upon addition of the more mobile CPOE, reach a minimum around 20–40% CPOE, and then increase toward the value for the pure cyclic component. Thus, threaded conformations are present across the entire composition range. The deviations between the measured D_{blend} and the predictions from a binary mixing rule

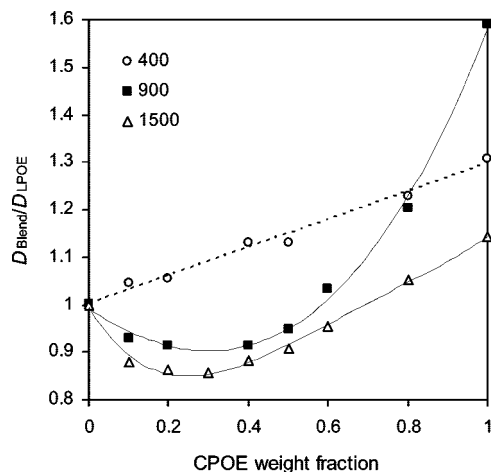


Figure 5. Ratio of self-diffusion coefficient of cyclic/linear blends of POE (same MW), D_{blend}/D , to D of the respective pure linear POE versus weight fraction of cyclic POE in the blend. Data measured at 56 °C for three blends: 400, 900, and 1500 g/mol. The dashed line represents weighted-average D_{blend} calculated from 400 g/mol pure-component D 's (eq 2); the solid lines are to guide the eye.

are greatest for the 1500 g/mol blend, indicative of the higher threading capability for this larger cyclic. For the POE blends composed of rings large enough to thread, the results shown in Figure 5 are consistent with those reported for blends of cyclic and linear DNA: $D_{C-C} > D_{L-C} > D_{L-L} > D_{C-L}$.^{7,8}

Assuming the D_{blend} reduction is related to the existence of threaded conformations, the equilibrium fraction of transient threaded species must be related to the magnitude of the deviation from the linear binary-mixing-rule prediction for a given blend composition. This implies that blends are composed of at least three species that coexist in dynamic equilibrium: free cyclic, free linear, and threaded chains. As a result, the average diffusion coefficient should be described by a three-term mixing rule:

$$D_{\text{blend}} = w_{\text{fc}}D_{\text{c}} + w_{\text{fL}}D_{\text{L}} + w_{\text{t}}D_{\text{t}} \quad (3)$$

where w_{fc} is the weight fraction of free (unthreaded) cyclic chains having D_{c} , w_{fL} is the weight fraction of free linear chains having D_{L} , and w_{t} is the weight fraction of threaded chains with diffusion coefficient D_{t} . Although multiply threaded species have been shown to exist by computational studies in cyclic/linear POE blends,¹² these will be ignored for the moment. If we assume that only threaded pairs of one linear chain and one cyclic chain exist, then $w_{\text{fc}} = w_{\text{c}} - 1/2w_{\text{t}}$ and $w_{\text{fL}} = w_{\text{L}} - 1/2w_{\text{t}}$, where w_{c} and w_{L} are the blend weight fractions of CPOE and LPOE, respectively. Since $w_{\text{L}} = 1 - w_{\text{c}}$, eq 3 can be simplified:

$$D_{\text{blend}} = (w_{\text{c}} - 1/2w_{\text{t}})D_{\text{c}} + (1 - w_{\text{c}} - 1/2w_{\text{t}})D_{\text{L}} + w_{\text{t}}D_{\text{t}} \quad (4)$$

According to eq 4, the blend diffusivity is a function of five different parameters: the weight fraction of cyclic in the blend, which is known from blend preparation; the diffusion coefficients of pure cyclic and linear polymers, which have been determined experimentally; and the unknown fraction of threaded pairs and their diffusivity, which are both unknown. None of the three species (characterized by D_{c} , D_{L} , D_{t}) are distinguishable in the PFG NMR data as monoexponential decays are observed for all of the blends. As demonstrated in Figure 2, if the component diffusivities are too similar, they will simply not be resolved in PFG echo attenuation plots. To find the missing parameters of w_{t} and D_{t} in the three-term mixing model, we prepared a series of CPOE/LPOE blends using deuterium-labeled linear POE (d-LPOE) and measured the self-diffusion

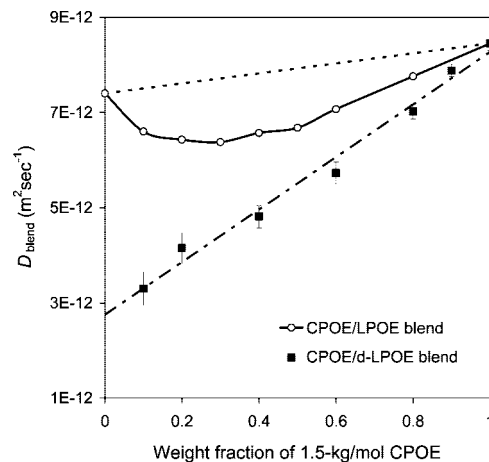


Figure 6. Self-diffusion coefficients vs weight fraction of 1.5 kg/mol CPOE for (a) fully hydrogenous blend with 1.5 kg/mol LPOE (○) and (b) hydrogenous-cyclic-only blend with 1.6 kg/mol deuterated LPOE (■). Data were measured at 56 °C. The dashed line represents the binary-mixing-rule prediction (cf. eq 2) for the fully hydrogenous blend. The dash-dotted line is a linear fit to the data for the hydrogenous-cyclic-only blend: $D_{\text{blend}} = 5.5 \times 10^{-12}w_{\text{c}} + 2.8 \times 10^{-12} \text{ m}^2/\text{s}$.

coefficients in these blends with PFG NMR. For these samples, the NMR signal arises solely from the protonated CPOE, thus allowing selective measurement of the average diffusion coefficient of cyclic components in the blend. The results are shown in Figure 6 as D_{blend} vs CPOE weight fraction for the fully hydrogenous blend (○) and the hydrogenous-cyclic-only blend (■). The diffusion data sets show sharp differences, thus providing proof that the monoexponential nature of the PFG echo decays is certainly not due to complete dynamic averaging of the components in these blends. The NMR signal for these hydrogenous-cyclic-only blends includes only contributions from free and threaded CPOE; the relative ratio of free and threaded CPOE at a given composition is contained in the measured D_{blend} . As the concentration of CPOE decreases (and the LPOE concentration increases), the concentration of threaded CPOE should increase, which is reflected in the data of Figure 6 as a continuous decrease in the average diffusion coefficient. By extrapolating to zero CPOE concentration, the trace diffusion coefficient for the CPOE in LPOE was determined to be $2.8 \times 10^{-12} \text{ m}^2/\text{s}$. If we take the extrapolated diffusion coefficient to be D_{t} , and using D_{c} and D_{L} measured on the neat melts, eq 4 can be used to calculate the weight fraction of threaded cyclic/linear pairs, w_{t} , as a function of CPOE concentration, w_{c} , from the D_{blend} values for the fully hydrogenous blends. The results of these calculations are shown in Figure 7 as w_{t} vs concentration of 1.5 kg/mol CPOE. The weight fraction of threaded chains reaches a maximum of ~ 0.25 at a CPOE concentration of 30–50%. Outside this CPOE concentration range, the weight fraction of threaded chains decreases due to the dilution of CPOE or LPOE.

The weight fraction of threaded chains was used with the CPOE concentration (w_{c}) to calculate the percentage of cyclics threaded: $100 \times (w_{\text{t}}/2)/w_{\text{c}}$. The factor 1/2 must be applied because w_{t} represents a threaded pair of one cyclic and one linear molecule. The linear scaling in Figure 6 supports the underlying hypothesis of eq 4 that CPOE exists either as free rings or as a threaded pair with LPOE. The % cyclics threaded are shown in Figure 8 as a function of CPOE concentration. As the blend progresses from LPOE-rich to CPOE-rich, the % cyclics threaded decreases smoothly from 87% at 10% CPOE to 6% at 80% CPOE. These data are qualitatively similar to those reported in two computational studies in that the percentage of cyclics threaded decreases as the blend moves from linear-rich to cyclic-rich.^{12,15}

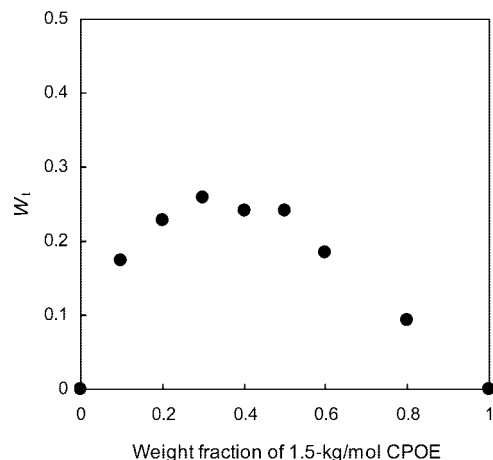


Figure 7. Weight fraction of threaded cyclic/linear pairs, w_t , vs CPOE weight fraction in the 1.5 kg/mol CPOE/LPOE blend, calculated using eq 4.

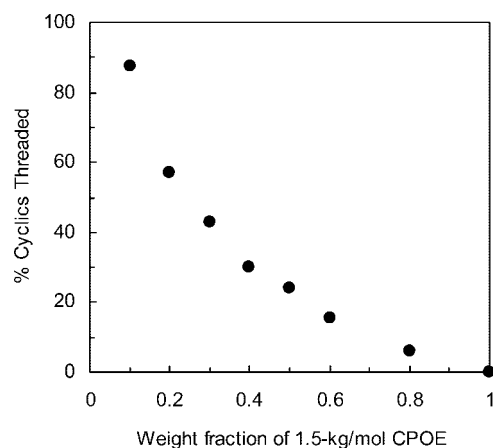


Figure 8. Percentage cyclics threaded vs CPOE weight fraction in the 1.5 kg/mol CPOE/LPOE blend, calculated from the data shown in Figure 7.

In the hydrogenous-cyclic-only blends, the NMR signal from free CPOE ($D_c = 8.8 \times 10^{-12} \text{ m}^2/\text{s}$; cf. Table 1) and threaded CPOE ($D_t = 2.8 \times 10^{-12} \text{ m}^2/\text{s}$) is averaged to yield a single-exponential echo attenuation decay. The ratio of these two diffusion coefficients, D_c/D_t , is about 3, which according to Figure 2 should be detectable in the NMR data, at least for 50:50 blends. The ratio of free to threaded CPOE is closest to 50:50 in the 20 and 30% CPOE blends (cf. Figure 8). Unfortunately, the echo attenuation plots for these samples, which contain only 20–30% hydrogenous material, are too noisy to distinguish two components. While some degree of dynamic averaging is expected, it cannot be determined from these data to what extent it occurs. Our threading analysis assumes no dynamic averaging since we use the pure-component D 's, and the results of the analysis agree well with published data on % cyclics threaded. For example, Helfer et al. modeled blends of equivalent-MW cyclic and linear POE with skeletal or backbone lengths of 24–60 atoms.¹² Consistent with numerous experimental reports on cyclic PDMS, they found that the % cyclics threaded increases with increasing ring size. Their data are shown in Figure 9 as % cyclics threaded vs number of cyclic backbone atoms for cyclic/linear POE blends containing 25% CPOE. Interpolated from our experimentally determined values at 20 and 30% 1.5 kg/mol CPOE, 50% cyclics threaded for a ring size of 100 atoms is shown in Figure 9 for comparison. Their simulated data can be fit to a second-order polynomial; if this is extended, it would suggest that our experimental

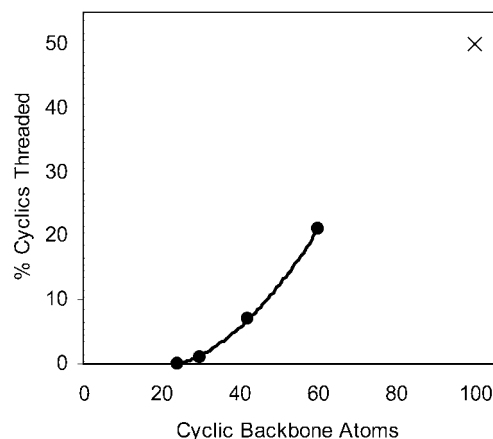


Figure 9. Percentage cyclics threaded vs number of cyclic backbone atoms for cyclic/linear POE blends at a cyclic concentration of 25%: (●) simulated data taken from the literature¹² and (×) interpolated from experimentally determined NMR self-diffusion data. Solid line is a second-order polynomial fit to the simulated data.

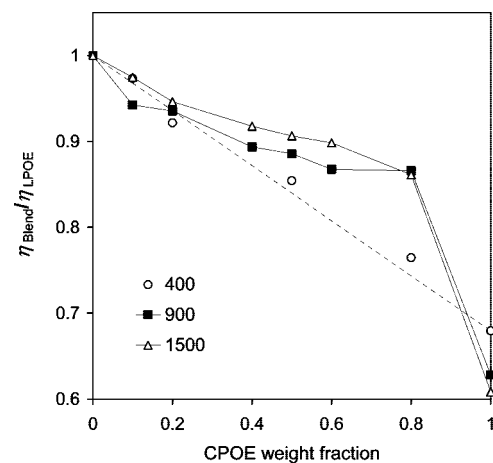


Figure 10. Ratio of zero-shear viscosity of cyclic/linear blends of POE (same MW), η_{blend} , to viscosity of the respective linear POE (η_{LPOE}) vs weight fraction of cyclic POE in the blend. Data measured at 56 °C for three blends: 400, 900, and 1500 g/mol. Dashed line represents weighted-average viscosity calculated from 400 g/mol pure-component viscosities.

determination is an underestimate of the % cyclics threaded for rings containing 100 atoms. However, the upward-concave shape to the data is not expected to persist. Network trapping of cyclic PDMS showed that the % cyclics threaded increases with ring size in a sigmoidal fashion.⁶ Assuming the cyclic POE behaves similarly, our experimental value in Figure 9 is in reasonable agreement with the simulated data of Helfer et al.

The composition dependence of the viscosity was also measured and is shown in Figure 10 for three different CPOE/LPOE blends: 400, 900, and 1500 g/mol. In analogy with the diffusion data in Figure 5, the ratio of blend viscosity to component LPOE viscosity ($\eta_{\text{blend}}/\eta_{\text{LPOE}}$) is plotted versus CPOE weight fraction. In agreement with the diffusion data, the 400 g/mol viscosity ratio changes linearly according to a simple binary mixing rule, while the larger cycles exhibit higher-than-predicted blend viscosities for CPOE concentrations greater than 20%. The greatest viscosity increases occur in blends that contain small quantities of linear chains (high fractions of cyclic). This dramatic effect of small quantities of linear chains on the viscosity of cyclic polymers has been observed previously^{2,3} and is an important reason for removing linear impurities before measuring the viscosity of cyclic polymer samples.

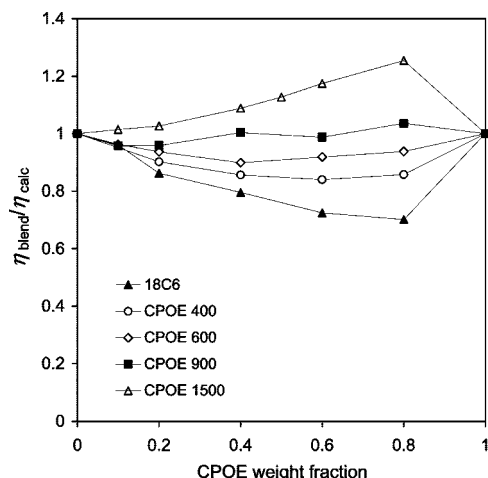


Figure 11. Ratios of experimental viscosities (η_{blend}) to viscosities calculated from the pure-component viscosities using a binary mixing rule (η_{calc}) vs weight fraction of cyclic POE (CPOE) for blends of 1500 g/mol linear POE with cyclic POEs of various molecular weights: 264 (18-crown-6), 400, 600, 900, and 1500 g/mol.

Stronger viscosity enhancement occurs in CPOE-rich blends while greater diffusion coefficient depression occurs in LPOE-rich blends. This can be rationalized by considering the nature of the two techniques and the structure of the cyclic/linear melt. Viscosity measurements probe dynamics under shear on time scales of seconds while diffusion NMR measurements are sensitive to center-of-mass translational dynamics in the milliseconds time regime. The different time scale sensitivities of diffusion vs viscosity measurements have been previously observed: For PDMS, reptation scaling of viscosity data is found above a characteristic molecular weight M_c , but not apparent in the diffusion data until much higher molecular weights ($>5M_c$).^{33,34} In the CPOE-rich blends, linear chains can thread through multiple cycles¹² which swells the cycles and increases ring–ring interactions;¹⁵ this extends the transient topological network beyond local cyclic/linear interactions, causing an increase in the viscosity. Subramanian and Shanbhag captured this very nicely in their bond-fluctuation model of cyclic/linear polymer melts.¹⁵ They found that the number of entanglements for the cyclic component increased with increasing linear concentration and approached (at high linear fraction) but never exceeded the number of entanglements for the linear component. This is consistent with our experimental observation that the blend viscosity never exceeds the viscosity of the pure LPOE (see Figure 10). They also found that the number of entanglements for the linear component was independent of blend composition, which means that any change in the dynamics in the LPOE-rich blends should be more localized, as is detected with diffusion measurements. Interdiffusion studies on polystyrene melts have revealed related behavior: for tracers into linear matrices (i.e., linear-rich blend), rings diffuse more slowly than linear chains;³⁵ for tracers into ring matrices (i.e., cyclic-rich blend), rings and linear chains diffuse at the same rate.³⁶

The 1500 g/mol linear POE was blended with smaller rings to examine their effects on the blend viscosity. The data are shown in Figure 11 as $\eta_{\text{blend}}/\eta_{\text{calc}}$ vs CPOE concentration, where η_{blend} is the experimentally measured blend viscosity and η_{calc} is the viscosity calculated using a binary mixing rule similar to eq 2 in which the D 's have been replaced with η 's. Data are shown for blends of the 1500 g/mol LPOE with CPOE of molecular weights 264 (18-crown-6), 400, 600, and 900, and 1500 g/mol. As already shown in Figures 4 and 10, the blend in which both components are 1500 g/mol exhibits viscosities that are greater than predicted by simply mixing two components with the viscosities listed in Table 2. However, none of the other

blends exhibit viscosity enhancements. Blending of 1500 g/mol LPOE with 18-crown-6, CPOE₄₀₀, and CPOE₆₀₀ results in viscosities that are lower than predicted, while blending with CPOE₉₀₀ resulted in viscosities that are identical (within experimental error) to the predictions. No viscosity enhancements are observed for the blends containing CPOE₆₀₀ and CPOE₉₀₀ even though these rings are large enough for threading to occur (see Figures 4, 5, and 10). The viscosity suppression is related to the efficient packing ability of the rings.⁴ For rings that are sufficiently large to enable threading, the packing effect is offset by threading and resultant ring swelling so that the viscosity increases. The balance is perfect for the CPOE₉₀₀/LPOE₁₅₀₀ blend across the entire composition range; the viscosity appears perfectly additive for this blend, but this is simply the result of these two counteracting effects.

4. Conclusions

Self-diffusion coefficients (D) and zero-shear viscosities (η) were measured for blends of cyclic poly(oxyethylene) (CPOE) and linear dihydroxy-terminated poly(oxyethylene) (LPOE) with molecular weights ≤ 1.5 kg/mol. For blends composed of CPOE and LPOE with equivalent molecular weights, topological threading causes suppression of self-diffusion coefficients and enhancement of viscosities beyond what is predicted by simple binary mixing rules when the component molecular weights are greater than 400 g/mol (~ 27 skeletal or backbone atoms).

The self-diffusion coefficients were determined from pulsed-field-gradient (PFG) NMR echo attenuation decays. For all blends, the NMR data could be fit to single exponentials from which characteristic average diffusion coefficients were extracted. No indication of individual component diffusion coefficients was apparent in the data. However, when PFG-NMR data were measured on a blend composed of perdeuterated LPOE and hydrogenous CPOE, the average D was lower than that measured on the fully hydrogenous blend. Thus, complete dynamic averaging does not occur in these blends; single average diffusion coefficients are measured due to the inability to resolve component diffusion coefficients that are too similar (factor $\leq \sim 3$).

Self-diffusion coefficients were measured as a function of blend composition. For the 1500 g/mol blend, D 's for the hydrogenous-cyclic-only blend were extrapolated to zero CPOE concentration to yield the trace D for CPOE in LPOE. This trace D was used for the threaded components with the pure-component D 's in a three-term mixing rule to determine the percentage of cyclics threaded. Consistent with published modeling studies,^{12,15} the % cyclics threaded decreased smoothly with increasing CPOE concentration. For 1500 g/mol CPOE, 50% are threaded at a ring concentration of 25%.

Acknowledgment. This work was supported in part by the National Science Foundation (DMR-0072876). We are grateful to Joyce Ferry for her assistance with cyclic polymer synthesis.

References and Notes

- (1) Antonietti, M.; Coutandin, J.; Grutter, R.; Sillescu, H. *Macromolecules* **1984**, *17*, 798–802.
- (2) McKenna, G. B.; Plazek, D. J. *Polym. Commun.* **1986**, *27*, 304–306.
- (3) Roovers, J. *Macromolecules* **1988**, *21*, 1517–1521.
- (4) Orrah, D. J.; Semlyen, J. A.; Ross-Murphy, S. B. *Polymer* **1988**, *29*, 1455–1458.
- (5) Cosgrove, T.; Turner, M. J.; Griffiths, P. C.; Hollingshurst, J.; Shenton, M. J.; Semlyen, J. A. *Polymer* **1996**, *37* (9), 1535–1540.
- (6) Clarson, S. J.; Mark, J. E.; Semlyen, J. A. *Polym. Commun.* **1986**, *27*, 244–245.
- (7) Robertson, R. M.; Smith, D. E. *Macromolecules* **2007**, *40* (9), 3373–3377.
- (8) Robertson, R. M.; Smith, D. E. *Proc. Natl. Acad. Sci. U.S.A.* **2007**, *104* (12), 4824–4827.

- (9) Cates, M. E.; Deutsch, J. M. *J. Phys. (Paris)* **1986**, 47, 2121–2128.
- (10) Pakula, T.; Geyler, S. *Macromolecules* **1988**, 21 (6), 1665–1670.
- (11) Arrighi, V.; Gagliardi, S.; Dagger, A. C.; Semlyen, J. A.; Higgins, J. S.; Shenton, M. J. *Macromolecules* **2004**, 37 (21), 8057–8065.
- (12) Helfer, C. A.; Xu, G.; Mattice, W. L.; Pugh, C. *Macromolecules* **2003**, 36 (26), 10071–10078.
- (13) Geyler, S.; Pakula, T. *Makromol. Chem., Rapid Commun.* **1988**, 9, 617–623.
- (14) Iyer, B. V. S.; Lele, A. K.; Shanbhag, S. *Macromolecules* **2007**, 40 (16), 5995–6000.
- (15) Subramanian, G.; Shanbhag, S. *Phys. Rev. E* **2008**, 77, 011801–9.
- (16) Wood, B. R.; Joyce, S. J.; Scrivens, G.; Semlyen, J. A.; Hodge, P.; O'Dell, R. *Polymer* **1993**, 34 (14), 3059–3063.
- (17) Gibson, H. W. Rotaxanes. In *Large Ring Molecules*; Semlyen, J. A., Ed.; J. Wiley and Sons: New York, 1996; Chapter 6, pp191–262.
- (18) Zhao, T.; Beckham, H. W.; Gibson, H. W. *Macromolecules* **2003**, 36 (13), 4833–4837.
- (19) DeBolt, L. C.; Mark, J. E. *Macromolecules* **1987**, 20, 2369–2374.
- (20) Joyce, S. J.; Hubbard, R. E.; Semlyen, J. A. *Eur. Polym. J.* **1993**, 29 (2/3), 305–312.
- (21) McLeish, T. *Phys. Today* **2008**, (August), 40–45.
- (22) Kapnistos, M.; Lang, M.; Vlassopoulos, D.; Pyckhout-Hintzen, W.; Richter, D.; Cho, D.; Chang, T.; Rubinstein, M. *Nat. Mater.* **2008**, 7, 997–1002.
- (23) McKenna, G. B.; Hostetter, B. J.; Hadjichristidis, N.; Fetters, L. J.; Plazek, D. J. *Macromolecules* **1989**, 22 (4), 1834–1852.
- (24) Singla, S.; Zhao, T.; Beckham, H. W. *Macromolecules* **2003**, 36 (18), 6945–6948.
- (25) Rubinstein, M.; Colby, R. *Polymer Physics*; Oxford University Press: New York, 2003; p 442.
- (26) Nam, S.; Leisen, J.; Breedveld, V.; Beckham, H. W. *Polymer* **2008**, 49, 5467–5473.
- (27) Yu, G.-E.; Sinnathamby, P.; Price, C.; Booth, C. *Chem. Commun.* **1996**, 1, 31–32.
- (28) Bates, F. S.; Fetters, L. J.; Wignall, G. D. *Macromolecules* **1988**, 21 (4), 1086–1094.
- (29) Singla, S.; Beckham, H. W. *Macromolecules* **2008**, 41, 9784–9792.
- (30) Stejskal, E. O.; Tanner, J. E. *J. Chem. Phys.* **1965**, 42, 288–292.
- (31) von Meerwall, E.; Ozisik, R.; Mattice, W. L.; Pfister, P. M. *J. Chem. Phys.* **2003**, 118 (8), 3867–3873.
- (32) Cosgrove, T.; Griffiths, P. C.; Webster, J. R. P. *Polymer* **1994**, 35 (1), 140–144.
- (33) Cosgrove, T.; Griffiths, P. C.; Hollingshurst, J.; Richards, R. D. C.; Semlyen, J. A. *Macromolecules* **1992**, 25 (25), 6761–6764.
- (34) Appel, M.; Fleischer, G. *Macromolecules* **1993**, 26 (20), 5520–5525.
- (35) Mills, P. J.; Mayer, J. W.; Kramer, E. J.; Hadziioannou, G.; Lutz, P.; Strazielle, C.; Rempp, P.; Kovacs, A. J. *Macromolecules* **1987**, 20 (3), 513–518.
- (36) Tead, S. F.; Kramer, E. J.; Hadziioannou, G.; Antonietti, M.; Sillescu, H.; Lutz, G.; Strazielle, C. *Macromolecules* **1992**, 25 (15), 3942–3947.

MA802294J